First principles study of reactions in alucone growth: the role of the organic precursor

ARTICLE

First Principles Study of Reactions in Alucone Growth: the Role of the Organic Precursor

Received 00th January 20xx,
Accepted 00th January 20x

DOI: 10.1039/x0xx00000x

Arbresha Muriqi and Michael Nolan*

Organic-inorganic hybrid materials are a unique class of materials with properties driven by the organic and inorganic components, making them useful for flexible devices. Molecular layer deposition (MLD) offers novel pathways for the fabrication of such hybrids by using inorganic metal precursors and the vast range of organic molecules with tunable properties. To investigate and understand the mechanism of growth a combination of theoretical and experimental data is needed. In this contribution, we present a first principles investigation of the molecular mechanism of the growth of hybrid organic–inorganic thin films of aluminium alkoxides, known as "alucones" grown by MLD. We explore the interactions between precursors by analyzing the MLD reaction products of the alumina surface terminated with $Al(CH_3)$ groups after the trimethyl aluminium pulse; this yields monomethyl-Al_2O_3 ($Al\text{-}CH_3\text{-}Al_2O_3$) and dimethyl- Al_2O_3 ($Al(CH_3)_2\text{-}\ Al_2O_3$) terminated surfaces. The organic precursors are ethylene glycol (EG), diethylene glycol (DEG), triethylene glycol (TEG) and tetraethylene glycol (FEG). A detailed comparison with alucones grown with ethylene glycol (EG) and glycerol (GL) precursors is presented to assist the interpretation of experimental findings regarding the differences in the hybrid films grown by EG and GL. The results show that Al-O formation with release of methane is favorable for all precursors. EG and GL can lie flat and create so-called double reactions through the reaction of the two terminal hydroxyl groups with the surface fragments. This phenomenon removes active hydroxyl sites for EG. However, for GL the third hydroxyl group is available and growth can proceed. This analysis shows the origin of differences in thickness of alucones found for EG and GL.

Introduction

Hybrid materials engineered at the molecular scale can display unique properties which arise as a result of the combination of the advantages of both the organic and inorganic components.[1][2][3][4][5] For example, the organic component can be designed for a particular property, such as a photochemically active organic molecule, while the inorganic component can be used to promote the stability. This class of materials can show excellent mechanical, thermal and optical properties which makes them very useful in many economically and socially relevant technological applications.[6][7] They are likely to have many applications in fields including optical devices,[8] photoluminescence,[9] protective coatings,[10] catalysis,[11] sensors,[12] etc. Key to the application of hybrid organic-inorganic materials is to have a suitable fabrication approach to allow a high level of control over the composition and properties. In recent years Molecular Layer Deposition, MLD, has been developed as an exciting approach for the fabrication of these hybrid organic-inorganic materials.[3][4][5][13][14] MLD can also be used to fabricate pure organic films like polyurea, polyamide, polythiourea, polyazomethine, and polyester where each MLD organic film is deposited via the denoted chemical linkage. [15][16][17][18] MLD is a film deposition approach based on sequential self limiting reactions of organic and inorganic precursors. MLD is therefore very close to Atomic Layer Deposition (ALD), which is widely used in multiple technologies.[19][20][21][22][23][24] The difference between MLD and ALD is in the precursor chemistry. Whereas ALD uses exclusively inorganic precursors to deposit solid materials, MLD uses bifunctional organic molecules in addition to the usual inorganic precursors to prepare hybrid materials.[25][26][27][28] Several MLD processes have been developed for hybrid organic-inorganic films based on metal precursors and organic alcohols to yield

[a] Tyndall National Institute, University College Cork, Lee Maltings, Dyke Parade, Cork T12 R5CP, Ireland
[b] Michael.nolan@tyndall.ie

metal alkoxide films which are described as "metalcones".[3][4][5][29][30] As a prototypical example, hybrid organic-inorganic thin films based on aluminium oxide can be produced using metal alkyls (trimethyl aluminium, TMA) and organic diols (ethylene glycol, hydroquinone) or triols (glycerol) as the inorganic and organic precursors, respectively. The resulting aluminum alkoxide materials have a composition that can be described by (−Al−O−R−O−)n where R is the organic species and this family of hybrid materials is generally known as "alucones".[31][32][33][34][35] Alucone films were deposited in Ref 34 using TMA as the metal precursor and ethylene glycol (EG) as the organic precursor. A proposed mechanism for the growth of alucone using EG is presented in Figure 1. In this scheme, a hydroxylated Al_2O_3 surface is exposed to TMA, new Al-O bonds are created with H transfer from the surface hydroxyls and CH_4 is released as a product, which is the usual reaction scheme using TMA in Al_2O_3 ALD. Depending on the number of CH_3 groups that react with the surface protons and are released as CH_4 products, the surface can be terminated with monomethyl Al_2O_3 (MMA-Al_2O_3) or dimethyl-Al_2O_3 (DMA-Al_2O_3) after the TMA pulse. The resulting surface is exposed to EG, a new Al-O bond forms, CH_4 is again released as a product, and the surface is potentially left covered with the terminal hydroxyl groups of the EG precursor. It is also possible, depending on coverage of MMA or DMA, that both hydroxyl groups of the molecule can react with the substrate, a so-called "double reaction", which then removes active hydroxyl groups. Repeating the cycle promotes the build up of organic-inorganic hybrid films with alternating layers of the oxide and organic components.

The Al center of TMA binds to the oxygen lone pair of EG by Lewis acid/base interactions.[34] A range of metalcones with metal oxide components using precursors from atomic layer deposition (ALD) have also been fabricated,[36][37][38][39][40] and the organic□inorganic composition can be adjusted by controlling the relative number of inorganic and organic half-cycles during deposition.[41] These metalcone alloys have tunable chemical, optical, mechanical, and electrical properties that may be useful for designing various functional films.[7][13]

As a further example, titanium-containing hybrid organic−inorganic films known as "titanicones" have been deposited using $TiCl_4$ as the metal precursor and diols and triols as organic precursors. [37][42][43][44] In Ref 37 titanicones were grown using $TiCl_4$ as the inorganic component and ethylene glycol (EG) and glycerol (GL) for the organic component. For titanicones grown with EG [37], *in situ* ellipsometry at a fixed temperature of 100 °C shows that growth terminates after 5 to 10 cycles, probably because both hydroxyls of EG react with the surface. At the same temperature, for growth with GL the thickness increases up to 25 cycles. This is because GL has a third hydroxyl group that can react with the inorganic precursor in the next pulse. Another group of hybrid coatings is the vanadium-based "vanadicones".[13][38] Vanadium oxides, in particular V_2O_5, are well-known electrode materials for lithium-ion batteries.[30] Vanadicones have been investigated by using tetrakisethylaminovanadium (TEMAV) precursors and EG and GL as organic precursors.[38] For the EG-based vanadicone film, growth slowed down during the first 10 cycles and at cycle 100, the growth per cycle dropped below 0.1 Å. The TEMAV/GL process, on the other hand, resulted in linear growth. After the first 10 cycles, the GPC stabilized to 0.7 Å and this rate remained stable for up to at least 500 cycles. Glycerol has an additional hydroxyl group compared to EG and is able to provide an extra reactive hydroxyl group in the case of a double reaction of the terminal hydroxyl groups with the surface so the growth proceeds. Hybrid inorganic-organic films called "tincones" are grown using tetrakisdimethylamino-tin (TDMASn) as the organic precursor with different diols and triols as organics precursors. Experimental work on tincones used TDMASn as the inorganic precursor and ethylene glycol (EG) and glycerol (GL) as organic precursors. For EG-based tincones, the growth decreased over the first 50 cycles. At a temperature of 100 °C the GPC was 0.1 □. For GL-tincones, the growth per cycle (GPC) was stable for up to 200 cycles. The GPC was 0.8 □ at a sample temperature of 100 °C. Similarly to titanicone and vanadicone, it is proposed that using EG, both terminal OH groups can react with the surface, resulting in a layer without active sites to react with the metallic precursor on the next pulse.[39] Several MLD processes have been reported for zincones: DEZ-EG(ethylene glycol),[40][45] DEZ–HQ(4-hydroquinone),[46][47] DEZ–THB(trihydroxybenzene)[48], DEZ–GL(glycerol), [36] QCM analysis of zincones grown using Diethyl zinc ($Zn(C_2H_5)_2$) and ethylene glycol (EG) indicate that the Zn hybrid films with EG undergo the double reaction where the terminal OH groups react with available -$Zn(-C_2H_5)$ surface sites. As for the other metalcones, this phenomenon effectively decreases the growth rate of the hybrid film.[45] Understanding the reactivity between functional organic molecules and organometallic precursors and the role of different alcohols is very important for the MLD process. First principles modelling using density functional theory (DFT) has been widely used in modelling of ALD but has seen much less use in MLD. In Ref [49], a

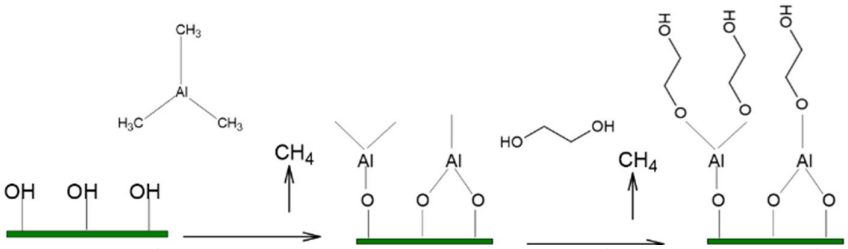

Figure 1 Schematic illustration of alucone MLD based on the reaction between surface hydroxyl groups of Al_2O_3 with TMA and the reaction between $Al(CH_3)$ and $Al(CH_3)_2$ surface species with EG.

hydroxylated silica (100) surface model was used to investigate the formation of MLD layers using TMA with phenol, 3-(trifluoromethyl)phenol, and 2-fluoro-4-(trifluoromethyl)-benzaldehyde, ozone (O_3) and hydrogen peroxide (H_2O_2). This work showed a continuation of the film growth in all three MLD processes where peroxyacid was formed in the reaction between carboxylic acid and hydrogen peroxide. According to the in situ FTIR measurements, the same peroxyacid structure was formed in the case of phenol, 3(trifluoromethyl)phenol and 2-fluoro-4-(trifluoromethyl)-benzaldehyde, at 100 °C. Interactions between trimethylaluminum (TMA) and the organic functional groups OH, NH_2, and NO_2 in the respective substituted phenyl molecules were carried out with DFT.[50] Reactions between TMA and all functional groups are favourable, but the dissociation of methyl groups from TMA requires an activation barrier to be overcome. These results indicate that the reactivity for TMA with NH_2 or NO_2 functional groups is lower than with OH. After deposition of the hybrid film, the most concerning practical issue for metalcones is their stability. This can be expedited by removal of the organic fragment of alucone layers by thermal annealing or mild water etching to produce a porous metal oxide network on the substrate surface.[51] These porous metal oxide films have been studied for hydrogen separation in composite membranes,[52] stabilization of Pt nanoparticles,[53] producing oxide and metal nanoparticles supported on Al_2O_3 nanotubes.[54]

Computational methods

We have used a three dimensional periodic slab model of α-Al_2O_3 modified with $Al(CH_3)_3$ species and the organic molecules described above within a plane wave basis set as implemented in the VASP5.4 code.[55] The valence electron-core electron interactions are described by the project augmented wave method,[56] with the following valance electron configurations: Al: $3s^23p^1$, O: $2s^22p^4$, C:$2s^22p^2$ and H:$1s^1$. The exchange-correlation functional is approximated by the Perdew–Burke–Ernzerhof (PBE) approximation.[57] The energy convergence criteria is E_{diff} = 1x10-4 eV and the geometry convergence criterion for the forces is E_{diffG} = $2x10^{-2}$ eV/Å. Alucone films were modelled using an α-Al_2O_3 slab from previous work.[58][59] The slab geometry was optimised by relaxing ionic positions, using an energy cut-off of 400 eV, and a Monkhorst-Pack k-point sampling grid of (3x3x1).[60] The computed equilibrium lattice parameters are a=b=9.614 Å c=25.25 Å and α = β=90° γ=120°. Interaction energies of the organic molecules with Al_2O_3 were calculated using:

$$E_{int}=\sum E_p-\sum E_r \quad (1)$$

E_p - Energy of products

E_r - Energy of reactants

For the example of the interaction of EG with DMA-Al_2O_3, $(CH_3)_2$-Al-Al_2O_3:

E_{int} = [E(EG-(CH_3)-Al-Al_2O_3)+E(CH_4)] – [E($(CH_3)_2$-Al-Al_2O_3)+(EG)]

The interaction energies for the other organic species and on MMA-Al_2O_3 are calculated in the same way. In exploring the diol-Al_2O_3 structures, we do not bias towards a particular Al coordination or symmetry. A negative E_{int} signifies an exothermic interaction and therefore the interaction is favourable.

Results

3.1 Surface models of TMA-terminated Al_2O_3 after the metal pulse

The hydroxylated surface of Al_2O_3 that results from the interaction with water and before the introduction of TMA is taken from previous studies on Al_2O_3.[58] Figure 2 shows the atomic structure of Al_2O_3 after the TMA pulse. The adsorption of TMA on a hydroxylated Al_2O_3 surface is a Lewis acid-base process and is barrier-free in the correct orientation: electrons are donated from oxygen of surface hydroxyls to the Al centre of the gas-phase TMA precursor. The adsorption energy includes contributions from formation of an Al-O bond and from associated tilting of the surface OH. We consider two possible terminations of Al_2O_3 after TMA pulse. The first is the monomethyl Al_2O_3 ($Al(CH_3)$-Al_2O_3, MMA-Al_2O_3) surface in which TMA has lost two CH_3 groups which have reacted with surface protons and are released as CH_4 molecules. Aluminium binds with two oxygens from the surface with distances of 1.76 Å for Al-$O_{(1)}$, 1.78 Å for Al-$O_{(2)}$ and 2.0 Å for Al-$O_{(3)}$. The surface therefore has one CH_3 group remaining that can react with the organic precursor in the next pulse. In the case of dimethyl-Al_2O_3 ($Al(CH_3)_2$-Al_2O_3, DMA-Al_2O_3) surface, TMA has lost one CH_3 group, released as CH_4 molecule. One new Al-O bond, with an Al-$O_{(1)}$ distance of 1.71 Å, is created. The surface has two CH_3 groups remaining that can react with the organic precursor in the next pulse. In addition to these models that result from the adsoprtion of a single TMA precursor we have also built models in which two $Al(CH_3)$ or two $Al(CH_3)_2$ species are adsorbed on Al_2O_3. The distance between the two aluminium sites in two adsorbed $Al(CH_3)$ is 2.64 Å while the surface model with two adsorbed $Al(CH_3)_2$ shows a distance of 4.18 Å between the two aluminium sites. These structures are shown in Figure 3.

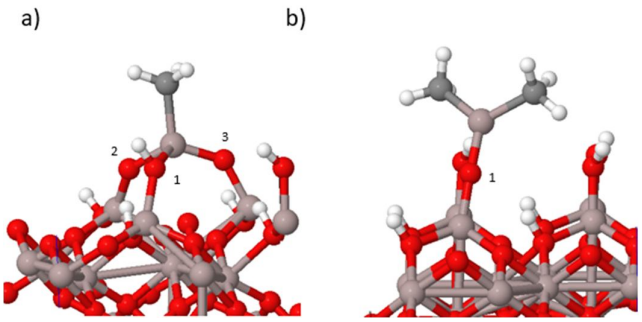

Figure 2 Atomic structure of (a) Monomethyl-Al-Al_2O_3 (Al-CH_3-Al_2O_3), (b) Dimethyl-Al-Al_2O_3 surface (Al$(CH_3)_2$-Al_2O_3). In this and all figures, the colour coding is as follows: Al-light grey spheres; O-red spheres; C- dark grey spheres; H-white spheres. The atom numbering is used in the text

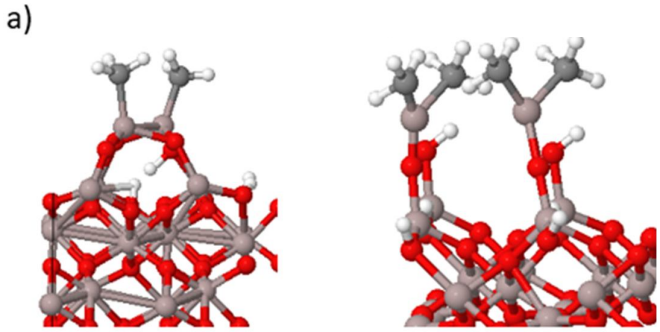

Figure 3 Atomic structure of (a) Two-MMA-Al_2O_3 surface 2(Al-CH_3)$_2$-Al_2O_3, (b) Two-DMA-Al_2O_3 surface 2(Al$(CH_3)_2$)-Al_2O_3. The colour coding is the same as Figure 2.

leading to hybrid films. In the case of DMA-Al_2O_3 surface the proton of the hydroxyl group of the organic precursor reacts with the CH_3 group of the TMA, to release a CH_4 molecule.

Table 1 Computed change in energy, from Equation (1), upon formation of Al-O bonds between MMA/DMA and the organic molecules of interest.

Structure	Interaction Energy (eV)
Dimethyl-Al_2O_3 – EG	-2.34
Dimethyl-Al_2O_3 – DEG	-1.82
Dimethyl-Al_2O_3 – TEG	-1.40
Dimethyl-Al_2O_3 – FEG	-1.48
Dimethyl-Al_2O_3 – GL	-2.17
Monomethyl-Al_2O_3 – EG	-1.54
Monomethyl-Al_2O_3 – DEG	-1.42
Monomethyl-Al_2O_3 – TEG	-1.48
Monomethyl-Al_2O_3 – FEG	-1.53
Monomethyl-Al_2O_3 – GL	-1.26

3.2 Reactions between organic precursors and MMA/DMA-terminated Al_2O_3

With these models of alumina in the post-TMA pulse, the interactions between the Al(CH_3) species and the organic precursors are then investigated by analyzing the formation of MLD reaction products with ethylene glycol (EG), diethylene glycol (DEG), triethylene glycol (TEG), tetraethylene glycol (FEG) and glycerol (GL). This set of organic precursors allows us to examine the influence of the chain length in the diol on the interaction between the O site of the molecules and the Al site of TMA, as well as the preferred orientation of the organic species. In addition, using glycerol allows us to compare a precursor with a third –OH group. The models with two MMA or DMA surface bound species allow us to study how favourable are "double reactions" of EG and GL, i.e. those reactions where the molecule tilts so that it binds to two Al(CH_3) species through the two terminal –OH groups. This is compared to the "single reaction" where the reaction takes place with one of the terminal –OH groups. Finally, we can use the results of this analysis to compare with experimental data on alucone growth. In our first calculations, all organic precursors were modeled in an up-right configuration. EG/DEG/TEG and FEG molecules contain two hydroxyl groups separated by a carbon chain and the hydroxyls serve as reactive linkers for condensation reactions with metal sites,

The computed change in energy upon forming the Al-O bond between one surface bound MMA/DMA on Al_2O_3 and the organic molecule is shown in Table 1. The resulting atomic structure is shown in Figure 4 for DMA and Figure 5 for MMA. From Table 1 we see that the formation of the Al-O bond between MMA/DMA and all diols, with release of CH_4, is favorable. The computed energy of interaction decreases with an increase of the chain length, going from -2.34 eV for EG to -1.48 eV for FEG, where we observe that there is little difference in the energy change on going from TEG to FEG.

We consider next the local geometry and in particular the Al-O distances between Al in MMA or DMA and the diol, as well as the Al-O distances to the surface. The Al-O distance could change when the length of the organic precursor is increased. Shorter Al-O bonds tend to be stronger, and this can effect the stability of the system. The resulting Al-O distance between Al in TMA and the alcohol increases when the chain length of the organic precursor increases. For the EG-DMA-Al_2O_3 surface, the Al-O distance is 1.73 Å and it lengthens slightly to 1.74 Å for the DEG-DMA-Al_2O_3 surface and to 1.75 Å for TEG-DMA-Al_2O_3 surface. However, for the FEG-DMA-Al_2O_3 surface there is a decrease to 1.73 Å. However, these changes are not particularly large and do not fully account for the wide change in interaction energy on going from EG to FEG.

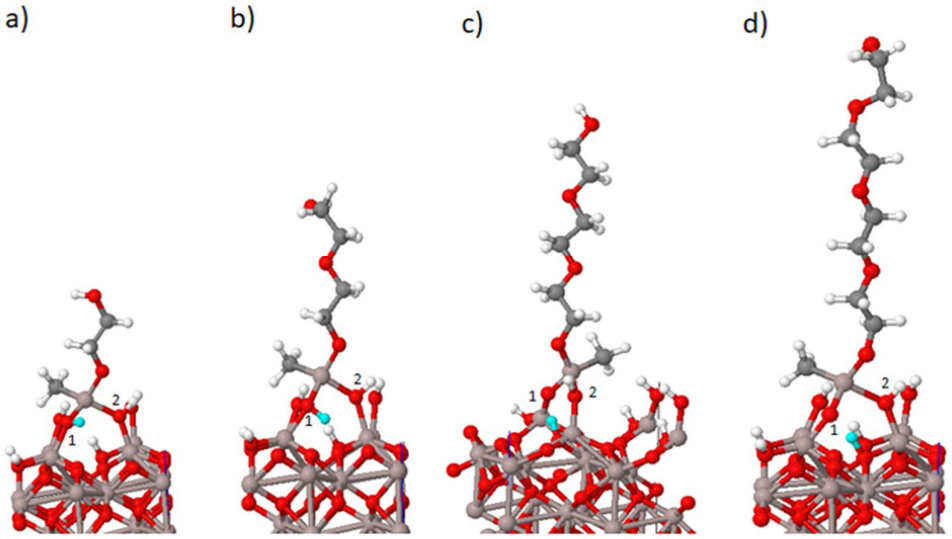

Figure 4 Atomic structures of MLD reaction products of the interaction of the DMA-Al_2O_3 surface with (a) ethylene glycol (EG), (b) diethylene glycol (DEG), (c) triethylene glycol (TEG) and (d) tetraethylene glycol (FEG). The transferred hydrogen is indicated by the cyan spheres and the atom numbering is used in the text.

When we compare the C-O and C-C distances between the free gas phase molecules and the same molecules bound to DMA/MMA, we also find little change; for example, the C-O distance in the free DEG is 1.40 Å and upon forming the bond to the DMA it changes to 1.41 Å.

The coordination number of Al can be affected by the reaction with the alcohol. In the DMA-Al_2O_3 surface, the Al is bound to one surface oxygen with an Al-O distance of 1.71 Å. When the diol is added this Al forms one more bond with another surface oxygen, resulting in a two coordinated Al site to surface O atoms, with a further bond to oxygen from the diol and C from the methyl group. For EG both Al-$O_{(1)}$ and Al-$O_{(2)}$ distances to the surface oxygens are 1.88 Å. For DEG the Al-$O_{(1)}$ distance is 1.83 Å and 1.92 Å for Al-$O_{(2)}$. For TEG and FEG the Al-$O_{(1)}$ distances are 1.73 Å and Al-$O_{(2)}$ distances are 2 Å. With the longer chains, Al-$O_{(1)}$ bond becomes shorter while Al-$O_{(2)}$ bond elongates. The oxygen of Al-$O_{(1)}$ also loses the hydrogen which transfers to another surface oxygen, as shown by the cyan sphere in Figure 4. This reduction in Al coordination in TEG and FEG compared to the shorter diols is consistent with the smaller energy gain upon formation of the new Al-O bond to the diol. Table 1 shows the computed interaction energies of MMA-Al_2O_3 with the organic diols and glycerol. In contrast to the computed energies at the DMA-Al_2O_3 surface, the interaction energies do not show a strong

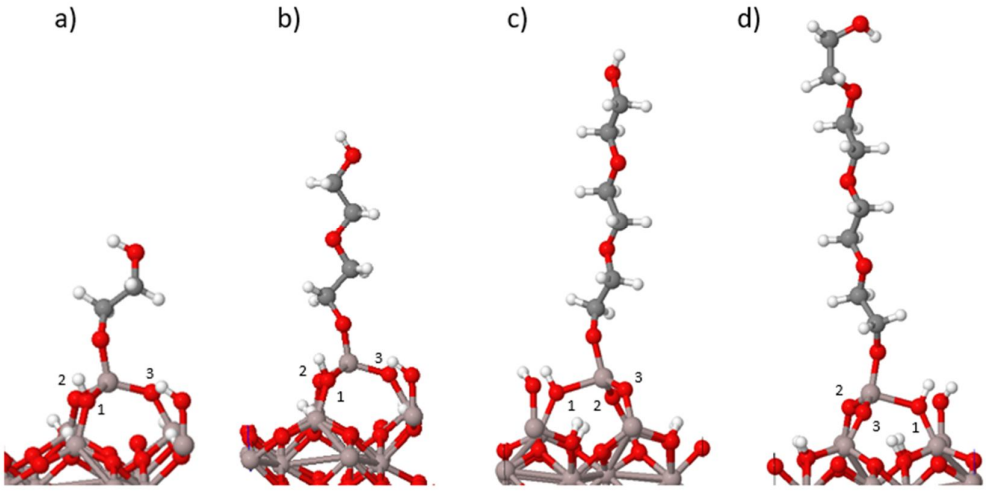

Figure 5 Atomic structures of MLD reaction products of the interaction of the MMA-Al_2O_3 surface with (a) ethylene glycol (EG), (b) diethylene glycol (DEG), (c) triethylene glycol (TEG) and (d) tetraethylene glycol (FEG). The atom numbering is used in the text.

dependence on the length of the diol, being -1.54 eV for EG and -1.53 eV for FEG. We suggest that this is due to the lack of the second methyl group in the Al_2O_3-MMA structure. In addition, Al-O distances to the alcohol are 1.72 Å in all cases, while the C-O and C-C distances are also not affected by the length of the molecule.

Table 2 Computed Al-O distances between MMA/DMA and the organic molecules of interest.

Structure	A-O distance (Å)
Dimethyl-Al_2O_3 – EG	1.73
Dimethyl-Al_2O_3 – DEG	1.74
Dimethyl-Al_2O_3 – TEG	1.75
Dimethyl-Al_2O_3 – FEG	1.73
Dimethyl-Al_2O_3 – GL	1.73
Monomethyl-Al_2O_3 – EG	1.72
Monomethyl-Al_2O_3 – DEG	1.72
Monomethyl-Al_2O_3 – TEG	1.72
Monomethyl-Al_2O_3 – FEG	1.72
Monomethyl-Al_2O_3 – GL	1.73

Examining the atomic structure for diol interactions at the MMA-Al_2O_3 surface, the coordination of the Al atom does not change with adding the diol, presumably arising in part to there being no methyl group present. Although the coordination number does not change, we do see some changes to the Al-O distances involving surface oxygen. Before adding the diol, the distances are 1.76 Å for Al-$O_{(1)}$, 1.78 Å for Al-$O_{(2)}$ and 2 Å for Al-$O_{(3)}$. The Al in MMA after adding the diol is coordinated to three surface O atoms and O from diol. For all diols the Al-Odistances from Al of MMA to the surface oxygens are 1.75 Å Al-$O_{(1)}$ and 1.77 Å Al-$O_{(2)}$. The distance to the third surface oxygen from a surface hydroxyl becomes longer, being in the range of 2.02 Å (for EG) to 2.05 Å (for FEG) Al-$O_{(3)}$.

Based on the interaction energies we propose that for longer diols it will be harder to maintain an upright configuration compared to lying flat and participating in the "double reaction" where the terminal –OH groups bind to the aluminium. However, the chain oxygens of DEG, TEG and FEG can also serve as active sites and they can bind with other TMA molecules. The adsorbed TMA molecules interact with new molecules of DEG, TEG or FEG and form three dimensional alucone networks [XX]. This highlights the complexity of alucone growth.

With DEG the growth rate increases when the chain length of the organic precursor is increased, even in the case of double reactions. [61] In the absence of chain oxygens in the organic precursor, because of the favoured double reactions that reduce the number of active sites from the surface (see section 3.3), we expect the growth rate to decrease when the carbon chain length is increased. This is in agreement with Ref. [62] where the thickness of alucones grown with ethanediol, butanediol and pentanediol varied with chain length. When the carbon chain length increased, the growth rate rapidly decreased and deviated from a linear pattern; and these changes were proposed to arise from the occurrence of a large number of double reactions, which resulted in the loss of reactive surface sites.

Due to the characteristic surface reaction of MLD, we have considered the secondary reaction between DMA terminated surface and EG. The interaction energy of DMA-Al_2O_3-2EG was calculated relative to the model of DMA-Al_2O_3-EG. Ethylene glycol (EG) molecules were modelled in an up-right configuration. Like for the primary reaction, again the proton of the hydroxyl group of EG reacts with CH_3 and produces a CH_4 molecule that is released as a by-product.

The computed change in energy upon forming the new Al-O bond between one surface bound DMA on Al_2O_3 and EG is -1.72 eV confirming that the secondary reaction is favourable. The Al-O distances to the alcohol molecules are 1.72 Å and 1.75 Å. When we compare Al-O distances with surface oxygens for DMA-Al_2O_3-2EG and DMA-Al_2O_3-EG we see some changes. While Al-$O_{(1)}$ and Al-$O_{(2)}$ distances in DMA-Al_2O_3-EG are 1.88 Å, for DMA-Al_2O_3-2EG the Al-$O_{(1)}$ distance decreases to 180 Å while Al-$O_{(2)}$ distance increases to 1.89 Å. It is reasonable that these EG species would also participate in the flat-lying reaction with a neighbouring DMA.

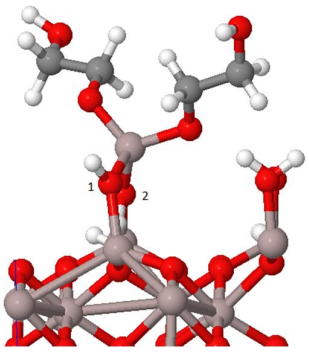

Figure 6 Atomic structures of MLD reaction products of the interaction of the DMA-Al_2O_3 surface with two ethylene glycol (EG) molecules. The atom numbering is used in the text.

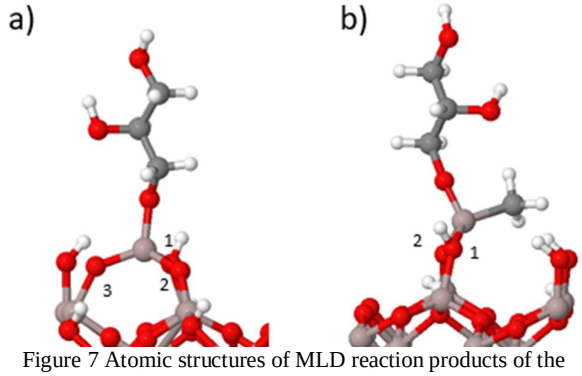

Figure 7 Atomic structures of MLD reaction products of the interaction of the (a) MMA-Al_2O_3 surface with glycerol (GL), (b) DMA-Al_2O_3 surface with glycerol (GL). The atom numbering is used in the text.

We now consider the interaction between the triol glycerol with the MMA/DMA-terminated Al_2O_3 surfaces. Again, glycerol (GL) was modelled in an up-right configuration. On both DMA-Al_2O_3 and MMA-Al_2O_3 surfaces, the proton of the hydroxyl group of glycerol reacts with CH_3 to produce a free CH_4 molecule released as the product while oxygen binds with the aluminium site. From the energetics in Table 1, we see that the formation of an Al-O bond is favourable in both cases.

Table 3 Computed Interaction Energy, from Equation (1), upon formation of Al-O bonds between MMA/DMA in the upright configuration of EG and GL. The energy change between the flat (double reaction) and upright configurations is also presented

Structure	Interaction Energy (eV)
2MMA-Al_2O_3 – EG upright	-1.18
2DMA-Al_2O_3 – EG upright	-1.47
2MMA-Al_2O_3 – GL upright	-1.24
2DMA-Al_2O_3 – GL upright	-1.28
Structure	**E(Flat) – E(Upright) (eV)**
2MMA-Al_2O_3 – EG flat	-1.49
2DMA-Al_2O_3 – EG flat	-1.42
2MMA-Al_2O_3 – GL flat	-1.03
2DMA-Al_2O_3 – GL flat	-1.17

).

However, the computed interaction energies is weaker on MMA-Al_2O_3-GL compared to DMA-Al_2O_3-GL; this difference is *ca.* 0.9 eV. The Al-O distances to the alcohol are 1.73 Å for both cases. The Al in MMA binds to three surface oxygen atoms with distances 1.75 Å for Al-$O_{(1)}$, 1.77 Å for Al-$O_{(2)}$ and 2.05 Å for Al-$O_{(3)}$. In DMA Al binds to two surface oxygen atoms with distanc1.88 Å for Al-$O_{(1)}$ and 1.90 Å for Al-$O_{(2)}$. These are similar to aluminium to surface oxygen distances for the diols. The C-O and C-C distances between the gas phase molecules and the molecules bound to DMA/MMA are little changed as a result of this interaction. The C-O distance in free glycerol is 1.42 Å and it changes to 1.41 Å upon binding to Al in DMA –Al_2O_3 and 1.40 Å in MMA-Al_2O_3.

3.3 Comparison of upright and flat-lying reactions of ethylene glycol and glycerol

To assist the interpretation of the experimental findings of the difference of the hybrid films grown with EG and GL [31][37][38] we investigate the models of Al_2O_3 terminated with two MMA or two DMA and examine the upright and flat lying or double reaction configurations of EG and GL. In the former, the molecules bind to one Al species through one terminal oxygen site, while in the latter the molecule binds through the two terminal oxygen sites to two neighbouring Al sites. Firstly, examining the geometry of the 2MMA and 2DMA termianted surfaces, the distance between the two aluminiums on 2MMA-Al_2O_3 is 2.64 Å and 4.18 Å on the 2DMA-Al_2O_3 surface. This geometry is geometrically favourable for the EG molecules to lie flat, with a distance of 3.69 Å between the terminal oxygen sites in EG and in this way both active groups of EG will be occupied. The distance

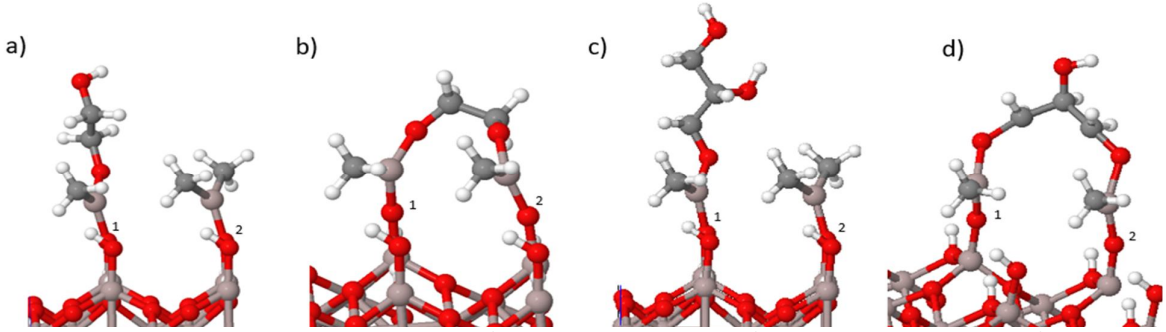

Figure 8 MLD reaction products at the 2-DMA-Al_2O_3 surface with (a) upright EG, (b) flat EG, (c) upright GL and (d) flat GL. The atom numbering is used in the text.

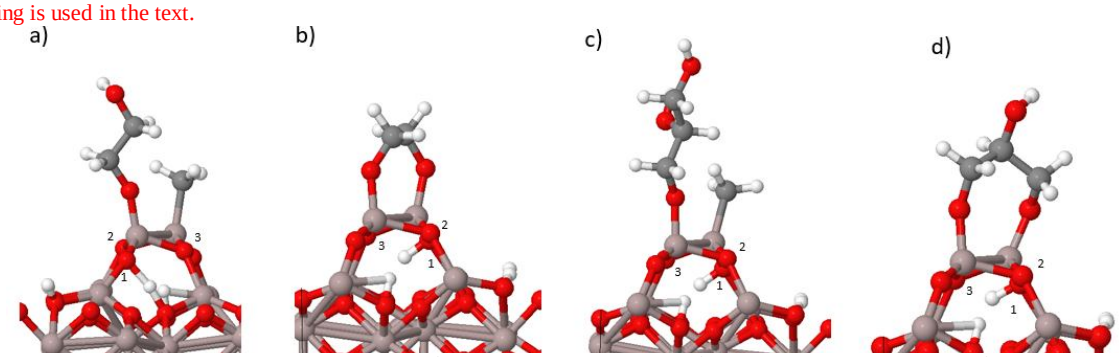

Figure 9 MLD reaction products at the 2-MMA-Al_2O_3 surface with (a) upright EG, (b) flat EG, (c) upright GL and (d) flat GL. The atom numbering is used in the text.

between the oxygen sites in the gas phase GL molecule, 4.98 Å, is also long enough to create double reactions with the MMA/DMA sites on the Al_2O_3 surface. However, in contrast to EG, GL has a third hydroxyl group, and this group will not be used in the binding in the flat lying configurations, so that it can persist as a reactive group irrespective of how the molecule binds. This hydroxyl can then react with TMA in a subsequent metal pulse. We compute the energy change when the organic molecules bind to one Al site in an upright configuration and these energies are shown in Table 3. The GL molecule interacts in an upright configuration with an energy gain of -1.25 eV at both 2MMA-Al_2O_3 and 2DMA-Al_2O_3, while for EG there is a difference of 0.3 eV between interaction at MMA and DMA. However, all interactions are favourable for both molecules and the resulting atomic structures are shown in Figures 8 (a) and (c) for DMA and Figure 9 (a) and (c) for MMA.

Table 4 Computed Al-O distances between MMA/DMA and EG and GL in the upright and flat lying configurations.

Structure	Al-O distance (Å)
2MMA-Al_2O_3 – EG upright	1.68
2DMA-Al_2O_3 – EG upright	1.7
2MMA-Al_2O_3 – GL upright	1.71
2DMA-Al_2O_3 – GL upright	1.72
Structure	**Al-O distance (Å)**
2MMA-Al_2O_3 – EG flat	1.7
2DMA-Al_2O_3 – EG flat	1.68
2MMA-Al_2O_3 – GL flat	1.71
2DMA-Al_2O_3 – GL flat	1.71

From Table 3 we see that the formation of double reactions between MMA/DMA and ethylene glycol (EG) and glycerol (GL), together with release of CH_4,is favorable. The energies of the models with the flat laying precursors were then calculated relative to the models with the upright EG and GL. We compute an energy gain of between -1.03 and -1.49 eV, which means that the formation of Al-O bonds through both terminal hydroxyls of the organic precursor is favourable and preferred for both molecules. When we compare the Al-O distances between the upright models and flat lying models we see that the Al-O distances to the alcohol undergo only small changes. For EG-DMA, the Al-O distance decreases from 1.70Å for the upright model to 1.68 Å for the flat lying model while for GL-DMA the Al-O distance decreases from 1.72 Å for the upright model to 1.71Å for the flat lying model. A similar trend is seen on the MMA-terminated surface. For EG-MMA the Al-O distance increases from 1.68 Å for the upright to 1.70 Å for the flat-lying configuration. For GL-MMA-GL the Al-O distance is the same in both cases, 1.71 Å. For the upright EG and GL on the 2DMA-Al_2O_3 surface, Al-$O_{(1)}$ and Al-$O_{(2)}$ distances between Al of DMA and surface oxygens are 1.70 Å. For the flat lying EG and GL Al-$O_{(1)}$ and Al-$O_{(2)}$ distances to the surface are 1.69 Å. For the upright EG on the 2MMA surface, the distances between Al of MMA and surface oxygens are 1.63 Å for Al-$O_{(1)}$ 1.82 Å for Al-$O_{(2)}$ and 2.05 Å for Al-$O_{(3)}$. For the upright GL the distances are 1.74 Å for Al-$O_{(1)}$, 1.93 Å for Al-$O_{(2)}$ and 1.99 Å for Al-$O_{(3)}$. For the flat lying EG the Al-O distances are more uniform, being 1.85 Å for Al-$O_{(1)}$, 1.86 Å for Al-$O_{(2)}$ and 1.88 Å for Al-$O_{(3)}$ and indicative of a change of Al coordination to surface oxygen from 2-fold to 3-fold. For the flat laying GL the distances are 1.86 Å for Al-$O_{(1)}$ 1.88 Å for Al-$O_{(2)}$ and 1.90 Å for Al-$O_{(3)}$. Based on these energy differences, both terminal hydroxyl groups of EG and GL are able to react with surface bound DMA and MMA. For EG, the surface is left covered with no hydroxyl sites while with GL, the additional hydroxyl group is available for further reaction, which provides an atomistic origin for the findings of Ref.31, where linear and saturated growth was obtained in the temperature range of 100 °C to 145°C and a decrease in growth per cycle (GPC) with increasing temperature was observed for both processes. The decrease was less pronounced for the GL-based process which is also in agreement with the literature.[34][41]

3.4 Reaction of ethylene glycol and glycerol with trimethyl aluminium

In our final study, to examine the reactivity of flat-lying EG and GL with a TMA precursor molecule, we have built models where the remaining hydroxyl group of GL reacts with TMA and to form new Al-O bonds and a CH_4 molecule is released. These structures can be described as MMA-Al_2O_3-GL-MMA and DMA-Al_2O_3-GL-DMA, see Figure 10. For EG, we have also considered the reaction of TMA with the terminal oxygen sites, to assess if these sites are reactive towards the metal precursor and the structures are shown in Figure 11.

For GL, the energy gain in forming an Al-O bond with TMA, together with release of CH_4, is 1.36 eV for MMA and 1.63 eV for DMA. These are similar to the energy gains when forming the Al-O bond between MMA and GL indicating that this exposed hydroxyl group is reactive to TMA and further growth will proceed. For MMA-Al_2O_3-GL-MMA and DMA-Al_2O_3-GL-DMA the Al-O distance from the available –OH site and Al of the new TMA molecule is 1.69 Å. This is little changed from the Al-O distances of 1.69 Å and 1.70 Å for Al in the original surface bound MMA and DMA.

The energy gain in forming an Al-O bond between EG and TMA is -0.82 eV for MMA and -1.32 eV for DMA. These are smaller than the energy gains when forming the Al-O bond between the original exposed MMA/DMA and EG and we note that the TMA does not take an upright configuration. For MMA-Al_2O_3-EG-MMA and DMA-Al_2O_3-EG-DMA we see

some significant differences in the A-O distances. The Al-O distances from the organic to the adsorbed TMA molecule are

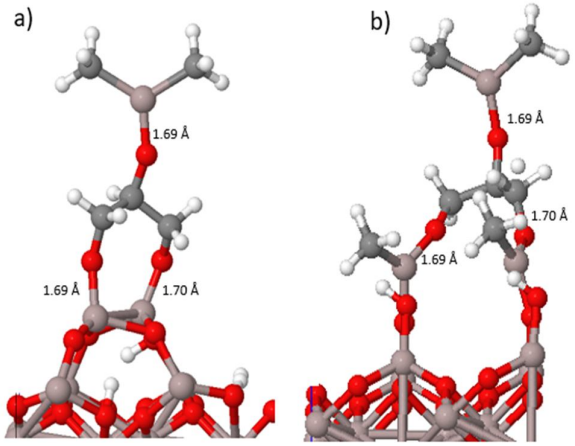

Figure 10 Atomic structure of (a) Flat-lying GL on MMA-Al_2O_3 surface with adsorption of TMA at the exposed OH site on GL, (b) Flat-lying GL on DMA-Al_2O_3 surface with adsorption of TMA at the exposed OH site on GL.

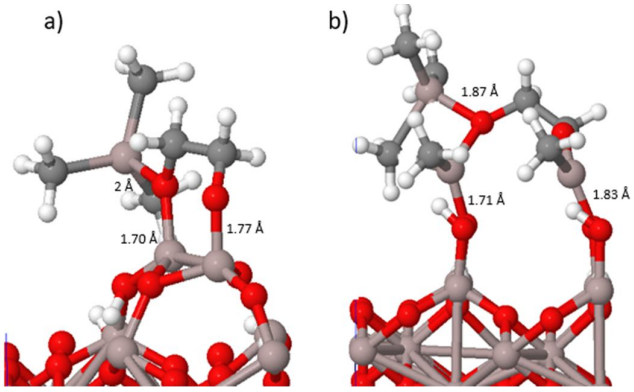

Figure 11 Atomic structure of (a) Flat-lying EG on MMA-Al_2O_3 surface with adsorption of TMA at the exposed O site on EG, (b) Flat-lying EG on DMA-Al_2O_3 surface with adsorption of TMA at the exposed O site on EG.

2.0 Å for MMA-Al_2O_3 and 1.87 Å for DMA-Al_2O_3 with less uniform Al-O distances of 1.71 and 1.83 Å involving the original DMA groups.

Consequently, we could expect that the growth can proceed, but the thickness of an EG alucone film would be smaller than that of a GL alucone film and this is consistent with experimental results in Ref. [31], where saturation curves show that TMA/GL MLD process gives higher growth rates per cycle and thicker films compared to the TMA/EG MDL process.

Conclusions

Organic-inorganic hybrid materials represent materials than can exploit the advantages of the different constituents, each with characteristic properties, which can deliver distinct advantages. Despite growing interest in these materials, there is little understanding of the atomistic mechanism of MLD film growth. In this study, the molecular mechanisms in the growth of hybrid organic–inorganic films, namely "alucones", which are based on trimethylaluminium (TMA) and various organic alcohols, is investigated through first principles density functional theory. We explored the interactions between the post-TMA pulse Monomethyl-Al_2O_3 (Al-CH_3-Al_2O_3, MMA-Al_2O_3) and Dimethyl-Al_2O_3 (Al(CH_3)$_2$-Al_2O_3, DMA-Al_2O_3) surfaces and different diols that differ by the length of chain. We found that the formation of the Al-O bond between MMA/DMA and all diols is favorable. However, for DMA-Al_2O_3 the energy gain decreases upon increasing the length of the diols. The longer the chain length the harder it is for the organic precursor to stay upright and we also find that the coordination of the Al atom from DMA changes on going from diethylene glycol to the triethylene glycol. In contrast to the computed energies at the DMA-Al_2O_3 surface, for MMA-Al_2O_3 surface the interaction energies are not affected by the diol length. The longer diols have oxygen sites avaialable along the chain which means that the growth mechanism and alucone structure with these longer diols will be complex [61,62] and this is as apsect worthy of further investigation.

The energetics of the reaction of a surface terminated with 2MMA or 2DMA species with ethylene glycol (EG) and glycerol (GL) show that while the organic precursors can bind to the TMA fragments via formation of Al-O bonds and loss of CH_4, it is most favorable for the organic precursors to lie flat and create so-called double reactions through the two terminal hydroxyl groups, where terminal oxygen sites bind to Al. For ethylene glycol, the surface is left with no hydroxyl sites and the growth will be less favorable while for glycerol, the third hydroxyl group is available for continued growth. We also showed that the TMA in the next pulse reacts favourably with this OH from GL and also terminal oxygen sites from EG, concluding that the growth can proceed for both. However, the GL-based alucone will grow thicker compared to the EG-based alucone as the energy gained from the interactions between TMA and the OH from GL is similar to the energy gained from MMA and GL. For EG-based alucone the energy gained from the interactions between TMA and oxygen sites is smaller compared with the energy gained from MMA and EG and the thickness of the resulting EG-TMA fragment is smaller than the GL-TMA fragment.

This study contributes to the understanding of growth process of EG-alucones and GL-alucones at the molecular level and is valuable in supporting experimental data on hybrid film growth.

Acknowledgement

We acknowledge support from H2020 MSCA-ITN Network HYCOAT, Grant Number 765378. We are grateful to Tyndall and the Irish Centre for High End Computing, ICHEC, for the provision of computing resources.

Conflicts of interest

There are no conflicts of interest to declare.

References

1. P. Judeinstein and C. Sanchez, "Hybrid organic-inorganic materials : a land of multidisciplinarity Chemistry : Synthesis of Hybrid Materials," *Journal of Materials Chemistry*, vol. 6, no. 4, pp. 511–525, 1996.
2. P. Gomez-Romero, "Hybrid Organic–Inorganic Materials—In Search of Synergic Activity," *Advanced Materials*, vol. 13, no. 3, pp. 163–174, 2001.
3. X. Meng, "An Overview of Molecular Layer Deposition for Organic and Organic-Inorganic," *Journal of Material Chemistry*, vol. 5, no. 35, pp. 1–53, 2017.
4. K. Gregorczyk and M. Knez, "Progress in Materials Science Hybrid nanomaterials through molecular and atomic layer deposition : Top down , bottom up , and in-between approaches to new materials,"*Progress in Material Science*, vol. 75, pp. 1–37, 2016.
5. P. Sundberg and M. Karppinen, "Organic and inorganic – organic thin film structures by molecular layer deposition : A review," *Beilstein Journal of Nanotechnology*, vol. 5, pp. 1104–1136, 2014.
6. F. Mammeri, L. Bourhis, and C. Sanchez, "Mechanical properties of hybrid organic – inorganic materials," *Journal of Materials Chemistry*, vol. 15, no. 35, pp. 3787–3811, 2005.
7. Y. Zhao and X. Sun, "Molecular Layer Deposition for Energy Conversion and Storage," *ACS Energy Letters*, vol. 3, no. 4, pp. 899–914, 2018.
8. Z-L. Xiaoa, H-Zh. Chena, M-M Shia, G. Wua, R-J. Zhoua, Zh-Sh. Yanga, M. Wanga, B-Zh. Tangb, "Preparation and characterization of organic–inorganic hybrid perovskite (C4H9NH3)2CuCl4," *Materials Science and Engineering B*, vol. 117, no.3, pp. 313–316, 2005.
9. Y. H. Li, H. J. Zhang, S. B. Wang, Q. G. Meng, H. R. Li, and X. H. Chuai, "Synthesis and luminescence properties of organic - inorganic hybrid thin films doped with Eu(III)," *Thin Solid Films*, vol. 385, no. 1, pp. 205–208, 2001.
10. K. Haas, K. Rose, and G. Schottner, "Functionalized coatings based on inorganic – organic polymers (ORMOCER A s) and their combination with vapor deposited inorganic thin films," *Surface and Coatings Technology* ,vol. 111, no. 1, pp. 72–79, 1999.
11. P. Battioni, E. Cardin, M. Louloudi, B. Schollhorn, G. A. Spyroulias, D. Mansuya and T. G. TrayIor, "Metalloporphyrinosilicas: a new class of hybrid organic-inorganic materials acting as selective biomimetic oxidation catalysts," *Chemical Communications*, vol. 17, pp. 2037–2038, 1996.
12. R. Makote and M. M. Collinson, "Template Recognition in Inorganic - Organic Hybrid Films Prepared by the Sol - Gel Process," *Chemistry of Mater* vol. 10, no. 9, pp. 2440–2445, 1998.
13. B. H. Lee, B. Yoon, A. I. Abdulagatov, R. A. Hall, and S. M. George, "Growth and Properties of Hybrid Organic-Inorganic Metalcone Films Using Molecular Layer Deposition Techniques," vol. 23, no. 5, pp. 532-546, *Advanced Functional Materials*, 2012.
14. D. M. King, X. Liang, and A. W. Weimer, "Functionalization of fine particles using atomic and molecular layer deposition," *Powder Technology*, vol. 221, pp. 13–25, 2012.
15. P. W. Loscutoff, H. Zhou, S. B. Clendenning, S. F. Bent, "Formation of Organic Nanoscale Laminates and Blends by Molecular Layer Deposition," *ACS Nanotechnology*, vol.4, no.1, pp 331–341, 2010.
16. N. M. Adamczyk, A. A. Dameron, and S. M. George "Molecular Layer Deposition of Poly(p-phenylene terephthalamide) Films Using Terephthaloyl Chloride and p-Phenylenediamine N," *Langmuir*, vol.24, no.5, pp. 2081-2089, 2008.
17. P.W. Loscutoff, H-Bo-R Lee, and S. F. Bent, "Deposition of Ultrathin Polythiourea Films by Molecular Layer Deposition," *Chemistry of Materials*, vol.22, no.19, pp. 5563–5569, 2010.
18. T.V. Ivanova, Ph. S. Maydannik, and D. C. Cameron "Molecular layer deposition of polyethylene terephthalate thin films," *Journal of Vacuum Science & Technology A*, vol.30, no.1, pp.01A121, 2012.
19. S. M. George, "Atomic Layer Deposition : An Overview," *Chemical Reviews*, vol. 110, no. 1, pp. 111–131, 2010.
20. M. Ritala, "Atomic layer deposition (ALD) : from precursors to thin film structures," *Thin Solid Films*, vol. 409, no.1, pp. 138–146, 2002.
21. B. S. Lim, A. Rahtu, and R. O. Y. G. Gordon, "Atomic layer deposition of transition metals," *Nature Materials*, vol. 2, no. 11, pp. 749–754, 2003.
22. R. W. Johnson, A. Hultqvist, and S. F. Bent, "A brief review of atomic layer deposition: From fundamentals to applications," *Matererials Today*, vol. 17, no. 5, pp. 236–246, 2014.
23. R. L. Puurunen, "Surface chemistry of atomic layer deposition: A case study for the trimethylaluminum/water process," *Journal of Applied Physics*, vol. 97, no. 12, pp.121-301, 2005.
24. S. D. Elliott, G. Dey, Y. Maimaiti, H. Ablat, E. A. Filatova, and G. N. Fomengia, "Modeling Mechanism and Growth Reactions for New Nanofabrication Processes by Atomic Layer

Deposition," *Advanced Materials*, vol. 28, no. 27, pp. 5367–5380, 2016.
25. M. Leskelä, M. Ritala, and O. Nilsen, "Novel materials by atomic layer deposition and molecular layer deposition," *MRS Bulletin*, vol. 36, no. 11, pp. 877–884, 2011.
26. S. H. Jen, B. H. Lee, S. M. George, R. S. McLean, and P. F. Carcia, "Critical tensile strain and water vapor transmission rate for nanolaminate films grown using Al2O3 atomic layer deposition and alucone molecular layer deposition," *Applied Physics Letters*, vol. 101, no. 23, pp. 2010–2013, 2012.
27. B. H. Lee, B. Yoon, V. R. Anderson, and S. M. George, "Alucone alloys with tunable properties using alucone molecular layer deposition and Al 2O 3 atomic layer deposition," *Journal of Physical Chemistry C*, vol. 116, no. 5, pp. 3250–3257, 2012.
28. H. Van Bui, F. Grillo, and J. R. Van Ommen, "Atomic and molecular layer deposition: off the beaten track," *Chemical Communication*, vol. 53, no. 1, pp. 45–71, 2017.
29. B. H. Lee, V. R. Anderson, and S. M. George, "Metalcone and Metalcone/Metal Oxide Alloys Grown Using Atomic and Molecular Layer Deposition," *The Electrochemical Society*, vol. 41, no. 2, pp. 131–138, 2011.
30. C. Ban and S. M. George, "Molecular Layer Deposition for Surface Modification of Lithium-Ion Battery Electrodes," *AdvancedMaterials Interfaces*, vol. 3, no. 21, 2016.
31. O. Al, K. Van De Kerckhove, M. K. S. Barr, and L. Santinacci, "The transformation behaviour of 'alucones', deposited by molecular layer deposition, in nanoporous Al2O3 layers," *Dalton Transactions*, vol. 47, pp. 5860–5870, 2018.
32. D. C. Miller, R. R. Foster, Sh-H. Jen, J. A. Bertrand, D. Seghete, B. Yoon Y-Ch Lee, S. M. George, M. L. Dunn, "Thermomechanical properties of aluminum alkoxide (alucone) films created using molecular layer deposition," *Acta Materiala*, vol. 57, no. 17, pp. 5083–5092, 2009.
33. D. Seghete, B. D. Davidson, R. A. Hall, Y. J. Chang, V. M. Bright, and S. M. George, "Sacrificial layers for air gaps in NEMS using alucone molecular layer deposition,"*Sensors and Actuators A: Physical*, vol. 155, no. 1, pp. 8–15, 2009.
34. A. A. Dameron, D. Seghete, B. B. Burton, S. D. Davidson, A. S. Cavanagh, J. A. Bertrand and S. M. George, "Molecular Layer Deposition of Alucone Polymer Films Using Trimethylaluminum and Ethylene Glycol," *Chemistry of Mater*ials, vol. 20, no. 10, pp. 3315–3326, 2008.
35. D. Choudhury, S. K. Sarkar, and N. Mahuli, "Molecular layer deposition of alucone films using trimethylaluminum and hydroquinone,"Journal of Vacuum Science & Technology A ,vol. 33, no. 1, p. 01-115, 2015.
36. J. J. Brown, R. A. Hall, P. E. Kladitis, S. M. George, and V. M. Bright, "Molecular layer deposition on carbon nanotubes," *ACS Nano*, vol. 7, no. 9, pp. 7812–7823, 2013.
37. H. V. Kerckhove, F. Mattelaer, D. Deduytsche, P. M. Vereecken, J. Dendoovena and Ch. Detaverniera, "Molecular layer deposition of "titanicone", a titanium-based hybrid material, as an electrode for lithium-ion batteries," *Dalton Transactions*, vol. 45, no. 3, pp. 1176 -1184, 2015.
38. K .V. Kerckhove, F. Mattelaer, J. Dendooven, and Ch. Detavernier, "Molecular Layer Deposition of "Vanadicone", a Vanadium-based Hybrid Material, as an Electrode for Lithium-ion Batteries" *Dalton Transactions*, vol. 46, no. 14, pp. 1176 -1184, 2017.
39. K. Van De Kerckhove, J. Dendooven, and C. Detavernier, "Annealing of thin ' Tincone ' fi lms , a tin-based hybrid material deposited by molecular layer deposition , in reducing , inert , and oxidizing atmospheres," *Journal of Vacuum Science & Technology A*, vol. 36, no. 5, 51-506, 2018.
40. Q. Peng, B. Gong, R. M. Vangundy, G. N. Parsons, and N. Carolina, " Zincone ' Zinc Oxide - Organic Hybrid Polymer Thin Films Formed by Molecular Layer Deposition," *Chemistry of Mater*ials, vol. 21. no. 5, pp. 820–830, 2009.
41. S. M. George, B. H. Lee, B. Yoon, A. I. Abdulagatov, and R. A. Hall, "Metalcones : Hybrid Organic – Inorganic Films Fabricated Using Atomic and Molecular Layer Deposition Techniques," *Journal of Nanoscience and Nanotechnology*, vol. 11, no. 9, pp. 7948-7955, 2011.
42. A. I. Abdulagatov, R. A. Hall, J. L. Sutherland, B. H. Lee, A. S. Cavanagh, and S. M. George, "Molecular Layer Deposition of Titanicone Films using TiCl 4 and Ethylene Glycol or Glycerol : Growth and Properties," *Chemistry of Materials*, vol. 24, no. 15, pp. 1–10, 2012.
43. A. I. Abdulagatov, K. E. Terauds, J. J. Travis, A. S. Cavanagh, R. Raj, and S. M. George, "Pyrolysis of Titanicone Molecular Layer Deposition Films as Precursors for Conducting TiO 2 / Carbon Composite Films," *The Journal of Physical Chemistry*, vol. 117, no. 34, pp. 17442-17450, 2013.
44. Zh. Song, M. Fathizadeh, Y. Huang, K. H. Chu, Y. Yoon, L. Wang, W. L. Xu, M. Yu "TiO2 nanofiltration membranes prepared by molecular layer deposition for water purification," *Journal of Membrane Science*, vol. 510, pp. 72–78, 2016.
45. B. Yoon, J. L. O'Patchen, D. Seghete, A. S. Cavanagh, and S. M. George, "Molecular layer deposition of hybrid organic-inorganic polymer films using diethylzinc and ethylene glycol," *Chemical Vapour Deposition*, vol. 15, no. 4–6, pp. 112–121, 2009.
46. B. Yoon, Y. Lee, A. Derk, C. Musgrave, and S. George, "Molecular Layer Deposition of Conductive Hybrid Organic-Inorganic Thin Films Using

Diethylzinc and Hydroquinone," *The Electrochemical Society*, vol. 33, no. 27, pp. 191–195, 2011.
47. B. Yoon, B. H. Lee, and S. M. George, "Highly Conductive and Transparent Hybrid Organic − Inorganic Zincone Thin Films Using Atomic and Molecular Layer Deposition," *The Journal of Physical Chemistry C*, vol. 116, no. 46, pp. 24784-24791, 2012.
48. K. S. Han and M. M. Sung, "Molecular layer deposition of organic-inorganic hybrid films using diethylzinc and trihydroxybenzene," *J. Nanosci. Nanotechnology*, vol. 14, no. 8, pp. 6137–6142, 2014.
49. L. Keskivali, M. Putkonen, E. Puhakka, E. Kentta, J. Kint, R. K. Ramachandran, Ch. Detavernier and P. Simell, "Molecular Layer Deposition Using Ring-Opening Reactions: Molecular Modeling of the Film Growth and the Effects of Hydrogen Peroxide ," *ACS Omega*, vol. 3, no. 7, pp.7141-7149, 2018.
50. F. Yang, J. Brede, H. Ablat, M. Abadia, L. Zhang, C. Rogero, S.D. Elliott, and M. Knez "Reversible and Irreversible Reactions of Trimethylaluminum with Common Organic Functional Groups as a Model for Molecular Layer Deposition and Vapor Phase Infiltration," *Advanced Materials Interfaces*, vol. 4, no. 18, pp. 170-237, 2017.
51. X. Liang, M. Yu, J. Li, Y. Jiang, and A. W. Weimer, "Ultra-thin microporous – mesoporous metal oxide films prepared by molecular layer deposition (MLD)," *Chemical Communications*, vol. 46, pp. 7140–7142, 2009.
52. M. Yu, H. H. Funke, R. D. Noble, and J. L. Falconer, "H2 Separation Using Defect-Free , Inorganic Composite Membranes," *Journal of the American Chemical Society*, vol. 133, no. 6, pp. 1748–1750, 2011.
53. T. D. Gould, A. Izar, A. W. Weimer, J. L. Falconer, and J. W. Medlin, "Stabilizing Ni Catalysts by Molecular Layer Deposition for Harsh, Dry Reforming Conditions," *ACS Catalysis*, vol. 4, no. 8, pp. 2714-2717, 2014.
54. Y. Qin, Y. Yang, R. Scholz, E. Pippel, X. Lu, and M. Knez, "Unexpected Oxidation Behavior of Cu Nanoparticles Embedded in Porous Alumina Films Produced by Molecular Layer Deposition," *Nano Letters*, vol. 11, no. 6, pp. 2503–2509, 2011.
55. G. Kresse and J. Furthmu, "Efficient iterative schemes for ab initio total-energy calculations using a plane-wave basis set ," vol. 54, no. 16, 1996.
56. P. Blochl, "Projector augmented-wave method," *Physical Review B*, vol. 50, p. 17953,1994
57. J. P. Perdew, K. Burke, and M. Ernzerhof, "Generalized gradient approximation made simple," *Physical Review Letters*, vol. 77, p. 3865, 28 October 1996.
58. G. R. Jenness, J. Seiter, and M. K. Shukla, "DFT investigation on the adsorption of munition compounds on α-Fe2O3: similarity and differences with α-Al2O3," vol. 20. no. 27, 2018.
59. G. N. Fomengia, M. Nolan, and S. D. Elliott, "First principles mechanistic study of self-limiting oxidative adsorption of remote oxygen plasma during the atomic layer deposition of alumina,"*Physical Chemistry Chemical Physics* , vol. 20, no. 35, pp. 22783–22795, 2018.
60. A. Hjorth Larsen, J. J. Mortensen, J. Blomqvist, I. E. Castelli, R. Christensen, M. Dulak, J. Friis, M. N. Groves, B. Hammer, C. Hargus, E. D. Hermes, P. C. Jennings, P. B. Jensen, J. Kermode, J. R. Kitchin, E. L. Kolsbjerg, J. Kubal, K. Kaasbjerg, S. Lysgaard, J. B. Maronsson, T. Maxson, T. Olsen, L. Pastewka, A. Peterson, C. Rostgaard, J. Schiotz, O. Schutt, M. Strange, K. S.Thygesen, T. Vegge, L. Vilhelmsen, M. Walter, Z. Zeng, and K. W. Jacobsen, "The atomic simulation environment-a Python library for working with atoms," *Journal of Physics-Condensed Matter*, vol. 29, p. 273002, 2017.
61. D. Choi, M. Yoo,H. M. Lee, J. Park, H. Y. Kim and J-S Park, "A Study on the Growth Behavior and Stability of Molecular Layer Deposited Alucone Films Using Diethylene Glycol and Trimethyl Aluminum Precursors, and the Enhancement of Diffusion Barrier Properties by Atomic Layer Deposited Al2O3 Capping," *ACS Applied Materials & Interfaces*, vol.8, no.19, pp.12263–12271, 2016.
62. Y-S Park, H. Kim, B. Cho, Ch. Lee, S-E. Choi, M. M. Sung and J. S. Lee,"Intramolecular and Intermolecular Interactions in Hybrid Organic − Inorganic Alucone Films Grown by Molecular Layer Deposition," *Applied Materials Interfaces*, vol. 8, no. 27, p. 17489-17498, 2016.

